ESSDD

Interactive
comment

Interactive comment on "A remote sensing-based dataset to characterize the ecosystem functioning and functional diversity of a Biosphere Reserve: Sierra Nevada (SE Spain)" *by* Beatriz P. Cazorla et al.

Beatriz P. Cazorla et al.

b.cazorla@ual.es

Received and published: 10 April 2020

Dear Reviewer,

Many thanks for your correspondence regarding our data description paper entitled "A remote sensing-based dataset to characterize the ecosystem functioning and functional diversity of a Biosphere Reserve: Sierra Nevada (SE Spain)". We thank you for all your constructive comments, which provided valuable insights to improve the conceptual and methodological robustness of our data and our paper. We are now very

[Printer-friendly version](#)

[Discussion paper](#)

pleased to send you the response to your comments and suggestions.

In our response below, please find our point-by-point responses (indicted with "R") presenting, in detail, how we have addressed the Reviewer comments ("C"). In the .pdf document attached, the Reviewer comments are reproduced in bold italic font and our responses are indicated in plain text, in addition, tables and figures are embed in the main document. We numbered each comment and reply for ease of reference and indicated changes that will be made in the manuscript.

Once again, we thank you for your time, constructive comments and suggestions. We hope to meet the expectations with this response, and that the Reviewer considers our data description manuscript suitable to be published in Earth System Science Data.

Sincerely,

The authors

Referee #1 Received and published: 23 March 2020 General comments: The authors provide a valuable compilation of remote sensing based indicators that are used to characterize the ecosystem condition of a test site in south-eastern Spain (Sierra Nevada). The indicators are computed from time series of Enhanced Vegetation Index (EVI) data from 16-day MODIS maximum value composite (MVC) data. The framework for the assessment of ecosystem functioning and functional diversity builds on a set of temporal metrics that are computed on an inter-annual, annual or seasonal level as well as on metrics that capture the spatial heterogeneity of the derived metrics. These metrics are used as proxies for ecosystem functional attributes (EFAs). The analysis of the temporal variability of the EFAs yielded the ecosystem functional types (EFTs) and the spatio-temporal heterogeneity of EFTs resulted in the characterization of ecosystem functional diversity. The main rationale behind this framework is that ecosystem primary production can be assessed from satellite vegetation indices and that primary production is the key indicator of ecosystem functioning. Overall, the proposed framework for computing EFTs and functional diversity from satellite time

series is comprehensible and well documented. The translation of temporal metrics of vegetation indices into functional attributes and type of ecosystems is well-founded and presents a prototype for large-scale ecosystem assessment and monitoring. The description of the datasets is appropriate and the data are available, structured and labelled logically. However, there are a few specific issues that need to be addressed before the manuscript can be accepted for publication:

Specific comments:

C1. - * The authors do not provide any information about the processing of the MODIS13Q1.006 time series to annual and inter-annual image stacks. Here, the most important point that has to be considered is the masking of valid pixels (clouds, aerosols, snow / ice, etc.) based on the quality assessment (QA) layer (VI Quality) of the MODIS dataset. The clarification on this issue is crucial has a direct impact on a number of the more technical comments below.

R1. - Thank you very much for raising this question. We used Enhanced Vegetation Index (EVI) since it minimizes canopy background variations and maintains sensitivity over dense vegetation conditions (Liu and Huete 1995). The MODIS EVI also uses the blue band to reduce residual atmosphere contamination caused by smoke and sub-pixel thin clouds (Huete et al. 1999). The MODIS EVI products are computed from atmospherically corrected bi-directional surface reflectances. Furthermore, the algorithm used by this product (MOD13Q1.006 product) chooses the best available pixel value from all the acquisitions from the 16 day period. The algorithm operates on a per-pixel basis and requires multiple observations (16 days) to generate a composited EVI. Due to orbit overlap, multiple observations may exist for one day and a maximum of four observations per day may be collected. The MOD13Q1 algorithm separates all observations by their orbits providing a means to further filter the input data.

Once all 16 days are collected, the MODIS algorithm applies a filter to the data based on quality, cloud presence, and viewing geometry (Fig. 1). Cloud-contaminated pixels

and extreme off-nadir sensor views are considered lower quality. A cloud-free, nadir view pixel with no residual atmospheric contamination represents the best quality pixel. Only the highest quality, cloud-free, filtered data are retained for compositing (Huete et al. 1999, Didan 2015b). The goal of the compositing methodology is to extract a single value per pixel from all the retained filtered data, which is representative of each pixel over the particular 16-day period. The compositing technique uses an enhanced criteria for normal-to-ideal observations, but switches to an optional backup method when conditions are less than ideal (Fig. 1).

The EVI values range from -1 to +1, where negative values generally correspond to snow, ice, or water; and values closer to +1 represent the higher density of green leaves (Huete et al. 2002). In our data, in addition to assuming the correct native pre-processing of the data explained above, negative values (associated with snow, ice or water) were transformed into zeros.

Despite the high standard quality of the 16-day EVI maximum value composite in MOD13Q1, we have assessed the effect of the additional application of the QA mask flags on the three Ecosystem Functional Attributes that are used as the basis for our further analyses and maps (e.g. the three metrics: EVI_mean, EVI_SD and EVI_DMAX). To do this, we have calculated EFAs using the "Summary Quality Assessment" band of MOD13Q1 product and masking out (values were substituted by NANs) the values 2: pixel covered with snow/ice, and 3: pixel cloudy. For EVI_mean and EVI_SD (continuous variables), and we carried out two comparisons: 1) we calculated a simple sliding window (3x3 pixels) correlation (Pearson correlation) between two rasters (data with QA mask and our data with negative values transformed into zeros), and plotted the map and histogram of the correlation coefficients (Fig. 2a-d), and 2)we calculated the linear regression between the filtered and unfiltered EFAs for the average year (Fig. 3). Most pixels had correlation values greater than 0.9, and the small areas with lower correlation between the filtered and non-filtered EVI_SD mainly occurred in oromediterranean belt, above the treeline. For EVI_DMAX, we assessed

the impact of masking by subtracting the filtered and unfiltered EVI_DMAX layers, once classified into seasons, to map the pixels that changed (mapped as 0) and those that did not change (mapped as 1) and to produce the corresponding histogram (Fig. 2e,f). Here, we only observed a small percentage of pixels with changes (4.35% of pixels changed and 95.65% did not change the EVI_DMAX season), located mainly in the oro- and crioromediterranean belts and the changes were from spring (with filtering using the QA mask) to summer (without QA mask). Therefore, the functional attribute less affected by the filtering was EVI_Mean, the one that has more weight in our data, the surrogate for primary production (see R8).

We also calculated linear regressions between the filtered and non-filtered, detecting a high relationship between both for EVI_mean (R=0.99), with slightly higher values of EVI for QA data (Fig. 3a) and a little more dispersion for EVI_sd (R=0.97), with lower values of sd for QA data (Fig. 3b).

Considering the small effect of filtering using the Quality Assessment bands on Ecosystem Functional Attributes and the very time-consuming effort that represents reprocessing all data, we have decided not to filter the dataset so far. However, if the reviewer and editor still think that we should apply the QA filtering, we will filter out snow, ice and water as zeros and clouds as NANs.

In case that the editor considers that no filtering is required, we would add the following text in the manuscript into section 2.2.

"MOD13Q1.006 EVI product is computed from atmospherically corrected bi-directional surface reflectances by choosing the best available pixel value from all the acquisitions (4 per day) in a 16 day period based on quality, cloud presence, and viewing geometry (Huete et al., 1999, Didan et al. 2015a). In addition, to further remove the potential remaining effect of snow, ice and water in our dataset, negative EVI values were transformed into zeros."

C2. - * If no masking has been carried out, the whole results section has to be revised.

R2. - Please, see response R1. We will provide comments (e.g. advantages and limitations) on this topic in the Discussion section of the manuscript after the open online discussion.

C3. - * The study area is rather small (2000 km2) and the landscape in the area shows small-scaled patterns of land-use patches. Why did you use coarse scale satellite data for your analysis and not the archive of available medium resolution satellite data (e.g. Landsat) for your work? This is more a general question, I do not really expect that you redo the full work, however, you could add a conclusive remark at the end of your work.

R3. - Thank you very much for your interesting question. Using MODIS instead of other satellites with higher spatial resolution (e.g. Landsat) has several advantages in terms of data quality (e.g. presence of clouds) along the time series. Since the MODIS sensor provides a daily image of the Earth, such high frequency (1 per day) increases the probability of finding a cloud-free image every 16-days (see response R1). MODIS provides the best composite value every 16 days (i.e. chooses the best available pixel value from all the acquisitions from the 16 day period), applying an algorithm that selects the image atmospherically corrected bi-directional surface reflectances and select the image with lowest cloud presence, the lowest view angle, and the highest EVI value (see response R1). Although Landsat has a lower pixel size, their images have a lower frequency (i.e., 1 image every 16 days). Thus, the fixed acquisition schedule makes it less probable to acquire good-quality imagery for a particular place periodically (especially if clouds occur frequently over the area of interest, e.g. winter dates).

Second, the Landsat product with the largest time series is Landsat 7 (1999-actually), however, on May 31, 2003, the satellite's scan-line corrector failed. The scan-line corrector is a device on the satellite that keeps the scan lines parallel to each other. Without the Scan Line Corrector (SLC), the scan lines are mis-aligned and there are wedge-shaped data gaps in the image (see sample Fig. 4 for Sierra Nevada). Providers offer different procedures for filling-in the data gaps, but each amounts to using data from good images prior to 2003 to do so. Obviously the further one gets from 2003,

the less valid this approach will be. Therefore, since 2003 SLC failure of Landsat 7, Landsat 8 is the only fully operational Landsat satellite in orbita, but covers a shorter time series than MODIS (Landsat8 covers from 2013 to actually, while MODIS covers from 2001 to actually).

Other satellites have also been considered for their use, as Sentinel, which also has a higher spatial resolution but the time series is still too short for long-term assessments (2014-present).

Finally, we consider appropriate MODIS spatial resolution for ecological studies at protected-area level, according to Anderson (2018), which showed that the temporal resolution of MODIS is useful for characterizing the seasonal dynamics of ecosystem functioning (Fig. 5). Furthermore, there are other works that use MODIS successfully at protected-area level (e.g. Lourenço et al. 2018, Requena-Mullor et al. 2018).

The arguments for the choice of MODIS were not included in the manuscript, therefore we would add the following sentence that briefly justify the choice of MODIS (section 2.2.): "Despite its moderate spatial resolution (aprox. 230 m/pixel), we chose MODIS since it offers a long time series (almost 20 years) of almost cloud-free images every 16 days thanks to the maximum value composite of daily images,which allows for the characterization of the temporal dynamics of ecosystem functioning (Anderson et al. 2018)".

Furthermore, we will also include comments in the Discussion section on the potential of extending our approach to Sentinel-2 data once the time-series gets longer.

Technical comments:

C4. - * Line 126: explain EVI and add reference

R4. - We chose EVI instead of any other vegetation index (such as SAVI, ARVI, or NDVI) as an indicator of carbon gains since it is supposed to be more reliable in both low and high vegetation cover situations (Huete et al. 1997). EVI is sensitive

to changes in areas having high biomass, EVI reduces the influence of atmospheric conditions on vegetation index values, and EVI corrects for canopy background signals (see R1).

EVI is computed following this equation:

EVI=G(NIR-red)/ (NIR+C1*red-C2*blue+L),

where NIR/red/blue are atmospherically-corrected (Rayleigh and ozone absorption) surface reflectances, L is the canopy background adjustment that addresses non-linear, differential NIR and red radiant transfer through a canopy, and C1, C2 are the coefficients of the aerosol resistance term, which uses the blue band to correct for aerosol influences in the red band. The coefficients adopted in the MODIS-EVI algorithm are; L=1, C1 = 6, C2 = 7.5, and G (gain factor) = 2.5.

We will explain EVI with its reference in the manuscript in section 2.2.

C5. - * Line 130: linked site is not available

R5. - Thank you for pointing it out. We will replace the old link with the updated one (https://lpdaac.usgs.gov/products/mod13q1v006/) (Didan 2015a).

C6. - * Line 130/131: the doi is not related to GEE. Please adjust accordingly either the link or the description.

R6. - Ok, thank you. We will modify the line by adding the official GEE reference: "Gorelick, N., Hancher, M., Dixon, M., Ilyushchenko, S., Thau, D., & Moore, R. (2017). Google Earth Engine: Planetary-scale geospatial analysis for everyone. Remote Sensing of Environment."

C7. - * Line 131/132: EVI between 0 and 1000 – in tables you use scaling from 0-1; what about negative values? The full data range is from -1 to +1.

R7. - Thank you for your comment. We transformed all negative values into 0, since negative EVI values are known to be related to the presence of snow, ice or water (and

therefore, ecologically, it makes more sense to have an EVI value of zero rather than negative) (Huete et al. 2002). In the new version, we will add an explanation about this in section 2.2 (see R1).

C8. - * Line 135/136: How did you identify these 3 metrics? There are a number of additional phenological metrics available that are known to represent meaningful features of ecosystem productivity (e.g. start / end, length of season). What is "biologically meaningful" in the context of your research?

R8. - Biologically, these three metrics can be interpreted as surrogates (Paruelo et al. 2001, Pettorelli et al. 2005, Alcaraz-Segura et al. 2006) of the total amount and timing (seasonality and phenology) of primary production, on of the most integrative indicators of ecosystem functioning (Virginia and Wall 2001). Statistically, these three metrics are known to be highly correlated with the first two or three axes (and hence capture most of the variance) of a Principal Component Analysis (PCA) carried out on the NDVI or EVI annual dynamics in different regions (Townshend et al. 1985, Paruelo and Lauenroth 1998, Paruelo et al. 2001, Alcaraz-Segura et al. 2006, Alcaraz-Segura et al. 2009, Ivits et al. 2013). To know the statistical meaningfulness of these metrics in Sierra Nevada Biosphere Reserve, we also examined their correlation with the first axes of a PCA run on the EVI annual curve of the average year (12 EVI values, i.e. the interannual means of the the maximum value composites for each month). The first two axes cumulated 96.5% of the variance (PC1 87.3%, PC2 9.2%). The eigenvectors showed that the weights along the months were similar for the first PCA axis (even weights throughout the year), while for the second axis they showed a contrast between winter and summer months (Table 1). This indicated that PC1 can be related to the total or average amount of EVI, and that PC2 can be related to the intra-annual variability of EVI (Fig. 6).

In addition, we explored the correlation between the PCA axis and the EVI metrics (i.e., EFAs). The EVI metrics showed high correlation with the PCA axes. PC1 accounted for most of the total variance in the seasonal dynamics of the EVI (87.3%) and was strongly

correlated with the EVI annual mean (PC1 vs. EVI_Mean r = 0.94). PC2 accounted for 9.2% of the total variance (PC1 and PC2 cumulated 96.5% of total variance) and was related to seasonality and phenology metrics (as in Alcaraz-Segura et al. 2006, 2009) (PC2 vs. EVI_SD r = -0.75; PC2 vs DMAX_Sine = 0.67; PC2-vs DMAX_Cosine = -0.61) (Table 2). To correlate DMAX with the PC axes and keep the continuous nature of the annual period and the relative distance between months (i.e. December is as close to January as July is to June, that is, the distance between December (12) and January (1) is one month, not eleven months), we transformed months into polar coordinates. The entire circumference of a year was divided into 12 portions and each month was equated to an angle (30° for January and 360° for December). DMAX months were therefore characterised by their sine and cosine values.

In summary, PC1 was very highly correlated to EVI_Mean and then can be interpreted as annual primary production. PC2 shows a high contrast in the eigenvector values between winter and summer and is highly correlated with EVI_SD and with the Sine and Cosine components of DMAX, so it can be interpreted as a combination of seasonality (SD) and phenology (DMAX). Mathematically, it could be expressed as follows: PC2 = f(a*SD + b*DMAX_Sine + c*DMAX_Cosine + d + e) (Table 1 and 2), and the r-square of this multiple regression was 0.70.

In addition, the EVI metrics were orthogonal, since the correlation between them was low, so that each EVI metric contributed independently to explain the variance of the EVI time series (Table 3).

Hence, these three EVI metrics are both "biologically and statistically meaningful" since they are linked to essential biodiversity variables such as productivity, seasonality and phenology and capture most of the variability of the EVI annual dynamics, a surrogate of primary production dynamics (Monteith 1972), the most integrative indicator of ecosystem functioning (Virginia and Wall, 2001), and the basis for multiple ecosystem processes and services (Paruelo and others 2016).

We will include a summary of this analysis (PCA and correlations) in the manuscript to better justify the biological and statistical meaningfulness of our EFAs.

C9. - * Line 139/140: How did you define the growing season?

R9. - Here we refer to a conceptual more than a technical definition of the growing season, as the period of the year with greater vegetation activity compared to other periods of the year with lower vegetation activity (de Beurs and Henebry 2010, Henebry and de Beurs 2013).

C10. - * Line 147/148: I doubt that you will have EVImax in the winter period after clearing your EVI data for snow/ice, clouds, etc.

R10. - The values of EVImax that we have found can be explained by the changing conditions of the environmental controls of vegetation growth along Sierra Nevada. In the Mediterranean mountains, both summer drought and winter cold are known to be the limiting factors of vegetation growth (Alcaraz-Segura et al. 2009). In Sierra Nevada, temperature is the main limiting factor of biological activity at the highest altitudes (oro- and crioro-mediterranean bioclimatic belts, see Figure in response R14), where vegetation growth is centered in the summer months (high temperature and water availability from the thaw). However, lower altitudes, and particularly in the southern and eastern parts of Sierra Nevada (see Figure in response R14), have drier and warmer conditions, and vegetation activity is mainly constrained by water availability during the summer. In these areas, during the winter months, precipitation is greater and temperature is still mild (12-15 °C, Rivas-Martínez 1997) which allows for vegetation growth (Alcaraz-Segura et al. 2009). In addition, such environmental conditions in the drylands have shaped plant species adaptations that enhance peak winter greenness, due to their fast response to scarce water inputs (Cabello et al. 2012). This is the case of some of the meso- and thermo- mediterranean scrublands (e.g. Anthyllis terniflora scrublands) which are dominated by summer-deciduous or malacophilous plant species (e.g. Anthyllis cytisoides, A. terniflora) that develop their maximum foliage in

the mid-winter. Nevertheless, ecosystem functioning in these areas was considered as rare in the context of the whole reserve, presenting EFTs with maximum greenness in winter (Ba4, Aa4). Since these areas are at the lowest altitudes in the park, and are not affected by the snow, the data filtering will not affect their EVI max in the winter period.

Another interesting result for the winter EVI peaks that can also be related to the particular climatic conditions in Mediterranean areas, is the case of pine afforestations at the upper bioclimatic belts (mainly in the supramediterranean belt). In Sierra Nevada, the pine formations in these bioclimatic belts correspond mainly to Pinus sylvestris and Pinus pinaster plantations and occur in the North slope, where we have found the largest areas with winter EVI max. According to Aragonés et al. (2019), there is a generalised pattern in the warmest and driest Mediterranean areas (i.e. Iberian Peninsula), where growing seasons of pines begin in autumn and extend to the following spring, due to the mild winters. The dormant period for these formations occurs in summer, as a consequence of the prolonged water stress (Atzberger et al. 2013, Peñuelas et al. 2004, Verger et al. 2016). Aragonés et al. (2019) findings couple with the phenological patterns in the supra- and oromediterranean pine forest areas, showing maximum peaks of EVI in winter (Fig. 7). Hence, Mediterranean pine species differing in relation to the dates of phenological events of the northern hemisphere, where the typical growing season of the vegetation in the northern hemisphere, according to the NDVI phenological pattern, starts with the photosynthetic activity in spring, achieves its maximum at the beginning of summer, and ends in autumn, with a dormant period in winter.

C11. - * Line 161: "relative extension" - what do you mean, here? Share of area of EFTi within a defined area (moving window)?

R11. - Thank you for this comment, which can lead to misinterpretation. "Relative extension" means that, in order to calculate rarity, the abundance of each EFT (in terms of occupied surface) is relative to the most abundant. However, for a better understanding, we will rewrite this part and the phrase will be replaced by removing the word "relative": "EFT rarity was calculated as the extension of each EFT compared

C12

to the most abundant EFT"

Once we have the rarity value of each EFT (using Equation 1) (line 164), we assign to each pixel in the EFT map such value according to its EFT class. Hence, the original spatial resolution of the EFT rarity map is the same as the resolution of the EFT map (230 m).

C12. - * Line 162: "compared to the most abundant EFT" – in a defined area / window?

R12. - Compared to the most abundant EFT in the study area. We will add this clarification to the sentence in the manuscript as follows: "EFT rarity was calculated for each year as the relative extension of each EFT compared to the most abundant EFT in the study area (Equation 1)" (line 164).

C13. - * Line 218: "altitudinal patterns"- What about topographical patterns (aspect, slope)?

R13. Thanks for this comment. We talk about data referring to altitudinal patterns as an example of data description. In the revised version, we will include patterns related to topography. However, we consider that further formal analyses in this regard are beyond the scope of a descriptive data paper.

C14. - * Line 219 ff.: I cannot find any map of those bioclimatic belts for the study area. Hence, I am not able to follow the description of results. Please add a figure.

R14. - We are very thankful for this comment, which will allow a better reading of the results. In the new manuscript, we will modify Figure 1 in the manuscript to include: the delimitation of the Biosphere Reserve and the distribution of the main ecosystems (Pérez-Luque et al. 2019) and thermotype bioclimatic belts (Molero-Mesa and Marfil 2015). We have added the new Figure 1 here, it is Figure 8 on this letter.

C15. - * Line 235: "maximum greenness in winter" – see comment above, how would you explain a greenness peak in wintertime?

R15. - Please, see response R10.

C16. - * Line 254: "interannual variability ranged from 1 to 17 different EFTs over the 18-year period" - what is the contribution of data uncertainty / data quality in this context, e.g. the missing QA-masking on one side and the very low EVI values on the other hand?

R16. - We consider that the data quality has no significant effect on the interannual variability of EFTs in the study area. First, although the inter-annual variability ranged from 1 to 17 different EFTs over the 18-year period, that maximum value of EFT changes occurred in only two pixels of the study area. More than 90% of the study area showed less than 10 EFTs over the 18-year period, and only 3% of the study area showed more than 12 EFTs. More than 75% of the study area showed a variability from 1 to 8 different EFTs (Table 4). Furthermore, variability was greater in intermediate bioclimatic belts, e.g. the mesomediterranean or supramediterranean, where pixels are not so influenced by the snow, but are more exposed to varying limiting conditions among years, summer droughts some years and winter cold some others. Whereas in the highest bioclimatic belts (e.g. oro- crioromediterranean), where the presence of snow and clouds is greater and more regular, so data quality would have a greater influence, the interannual variability was lower.

Second, regarding the very low EVI values (i.e. negative values), we had already transformed all negative values into zeros (but it was not sufficiently explained in the manuscript), to remove the potential remaining effect of snow, ice and water (please, see R1). Thus, we do not expect a high effect of filtering snow, ice or water on interannual variability of EFTs.

Finally, considering the small effect of filtering using the Quality Assessment bands on Ecosystem Functional Attributes, we believe that filtering would not affect the interannual variability. However, if the reviewer and editor still think that we should apply the QA filtering, we will filter out snow, ice and water as zeros and clouds as NANs.

C17. - * Line 359: "geospatial data Sierra Nevada Park" – Where do you show these data?

R17. - This is just the shapefile with the boundaries of Sierra Nevada. We will rename it and we will also include the ecosystem and bioclimatic belt maps (please, see R14).

C18. - * Line 366: "Sierra Nevada Biosphere Reserve (SE Spain)" – show in map!

R18. - Thank you for your suggestion, we will add a new figure showing this one, see R14.

C19. - * Figure 1: It would be helpful for the interpretation of the EFA and EFT data to have a map of vegetation types rather than a simple snapshot from the ISS without any information on content and scale.

R19. - We will do that, see R14.

C20. - * Figure 3: the mean EVI is NOT the "area under curve"! This would rather be the cumulative EVI.

R20. - That's right, we will rewrite this sentence as follows: " EFAs were: the annual mean or the cumulative EVI, an estimator of annual productivity (EVI_mean), the EVI seasonal coefficient of variation, i.e. the differences between the minimum and the maximum EVI values, a descriptor of seasonality (EVI_sSD), and the date of maximum EVI, an indicator of phenology (EVI_DMAX)".

REFERENCES

Alcaraz, D., Paruelo, J., & Cabello, J. (2006). Identification of current ecosystem functional types in the Iberian Peninsula. Global Ecology and Biogeography, 15(2), 200-212.

Alcaraz-Segura, D., Cabello, J., & Paruelo, J. (2009). Baseline characterization of major Iberian vegetation types based on the NDVI dynamics. Plant Ecology, 202(1), 13-29.

Anderson, C. B. (2018). Biodiversity monitoring, earth observations and the ecology of scale. Ecology letters, 21(10), 1572-1585.

Aragones, D., Rodriguez-Galiano, V. F., Caparros-Santiago, J. A., & Navarro-Cerrillo, R. M. (2019). Could land surface phenology be used to discriminate Mediterranean pine species?. International Journal of Applied Earth Observation and Geoinformation, 78, 281-294.

Atzberger, C., Klisch, A., Mattiuzzi, M., & Vuolo, F. (2014). Phenological metrics derived over the European continent from NDVI3g data and MODIS time series. Remote Sensing, 6(1), 257-284.

Cabello, J., Alcaraz-Segura, D., Ferrero, R., Castro, A. J., & Liras, E. (2012). The role of vegetation and lithology in the spatial and inter-annual response of EVI to climate in drylands of Southeastern Spain. Journal of Arid Environments, 79, 76-83.

de Beurs, K. M., & Henebry, G. M. (2010). Spatio-temporal statistical methods for modelling land surface phenology. In Phenological research (pp. 177-208). Springer, Dordrecht.

Didan, K. (2015a). MOD13Q1 MODIS/Terra Vegetation Indices 16-Day L3 Global 250m SIN Grid V006 [Data set]. NASA EOSDIS Land Processes DAAC. Accessed 2020-03-25 from https://doi.org/10.5067/MODIS/MOD13Q1.006

Didan, K., Munoz, A. B., Solano, R., & Huete, A. (2015b). MODIS vegetation index user's guide (MOD13 series). University of Arizona: Vegetation Index and Phenology Lab.

Henebry, G. M., & de Beurs, K. M. (2013). Remote sensing of land surface phenology: A prospectus. In Phenology: An integrative environmental science (pp. 385-411). Springer, Dordrecht.

Huete, A. R., Liu, H. Q., Batchily, K. V., & Van Leeuwen, W. J. D. A. (1997). A comparison of vegetation indices over a global set of TM images for EOS-MODIS. Remote

sensing of environment, 59(3), 440-451.

Huete, A., Didan, K., Miura, T., Rodriguez, E. P., Gao, X., & Ferreira, L. G. (2002). Overview of the radiometric and biophysical performance of the MODIS vegetation indices. Remote sensing of environment, 83(1-2), 195-213.

Huete, A., Justice, C., & Van Leeuwen, W. (1999). MODIS vegetation index (MOD13). Algorithm theoretical basis document, 3(213).

Ivits, E., Cherlet, M., Horion, S., & Fensholt, R. (2013). Global biogeographical pattern of ecosystem functional types derived from earth observation data. Remote Sensing, 5(7), 3305-3330.

Liu, H. Q., & Huete, A. (1995). A feedback based modification of the NDVI to minimize canopy background and atmospheric noise. IEEE transactions on Geoscience and Remote Sensing, 33(2), 457-465.

Lourenço, P., Alcaraz-Segura, D., Reyes-Díez, A., Requena-Mullor, J. M., & Cabello, J. (2018). Trends in vegetation greenness dynamics in protected areas across borders: what are the environmental controls?. International Journal of Remote Sensing, 39(14), 4699-4713.

Molero Mesa, J. & Marfil, J.M. 2015. The bioclimates of Sierra Nevada National Park. Int. J. Geobot. Research 5: 1-11.

Monteith, J. L. (1972). Solar radiation and productivity in tropical ecosystems. Journal of applied ecology, 9(3), 747-766.

Paruelo, J. M., & Lauenroth, W. K. (1995). Regional patterns of normalized difference vegetation index in North American shrublands and grasslands. Ecology, 76(6), 1888-1898.

Paruelo, J. M., Jobbágy, E. G., & Sala, O. E. (2001). Current distribution of ecosystem functional types in temperate South America. Ecosystems, 4(7), 683-698.

[Printer-friendly version](#)

[Discussion paper](#)

Paruelo, J. M., Texeira, M., Staiano, L., Mastrángelo, M., Amdan, L., & Gallego, F. (2016). An integrative index of Ecosystem Services provision based on remotely sensed data. Ecological indicators, 71, 145-154.

Peñuelas, J., Filella, I., Zhang, X., Llorens, L., Ogaya, R., Lloret, F., ... & Terradas, J. (2004). Complex spatiotemporal phenological shifts as a response to rainfall changes. New Phytologist, 161(3), 837-846.

Pérez-Luque, A.J.; Bonet-García, F.J.; Zamora Rodríguez, R (2019). Map of Ecosystems Types in Sierra Nevada mountain (southern Spain). PANGAEA, https://doi.org/10.1594/PANGAEA.910176

Pettorelli, N., Vik, J. O., Mysterud, A., Gaillard, J. M., Tucker, C. J., & Stenseth, N. C. (2005). Using the satellite-derived NDVI to assess ecological responses to environmental change. Trends in ecology & evolution, 20(9), 503-510.

Requena-Mullor, J. M., Reyes, A., Escribano, P., & Cabello, J. (2018). Assessment of ecosystem functioning from space: Advancements in the Habitats Directive implementation. Ecological Indicators, 89, 893-902.

Townshend, J. R., Goff, T. E., & Tucker, C. J. (1985). Multitemporal dimensionality of images of normalized difference vegetation index at continental scales. IEEE Transactions on Geoscience and Remote sensing, (6), 888-895.

Verger, A., Filella, I., Baret, F., & Peñuelas, J. (2016). Vegetation baseline phenology from kilometric global LAI satellite products. Remote sensing of environment, 178, 1-14.

Virginia, R. A., Wall, D. H., & Levin, S. A. (2001). Principles of ecosystem function. Encyclopedia of biodiversity, 2, 345-352.

Please also note the supplement to this comment:
https://www.earth-syst-sci-data-discuss.net/essd-2019-198/essd-2019-198-AC1-

supplement.pdf

Interactive comment on Earth Syst. Sci. Data Discuss., https://doi.org/10.5194/essd-2019-198, 2020.
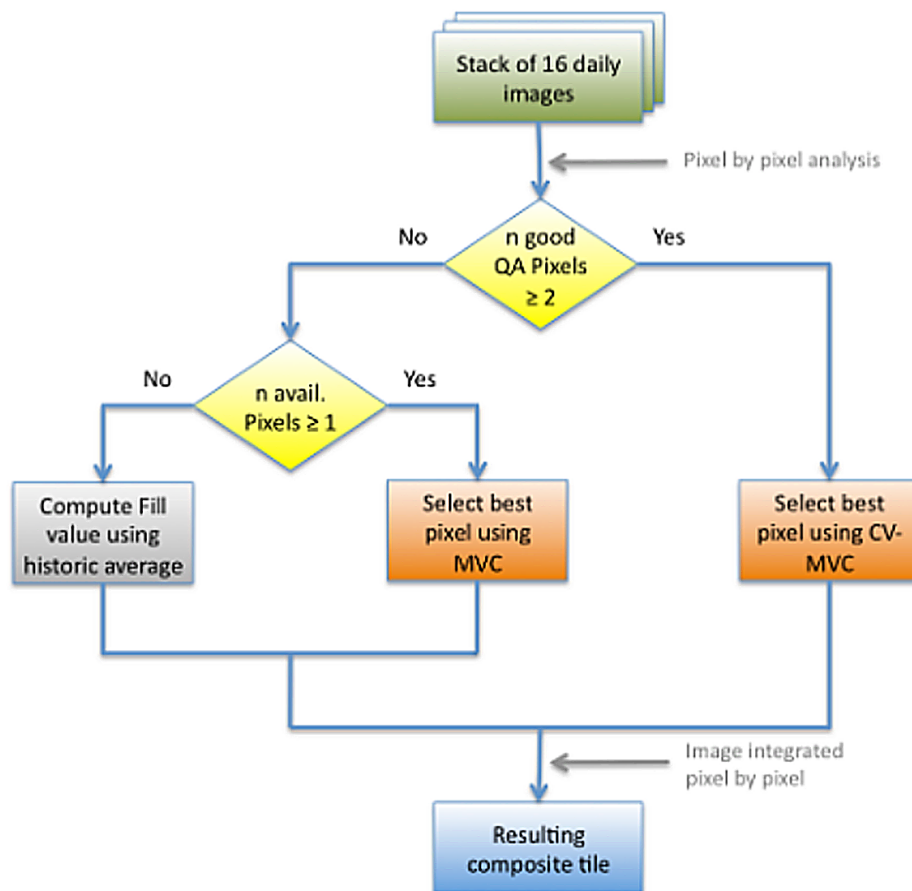
Fig. 1. MODIS compositing algorithm data flow (from Didan et al. 2015b).
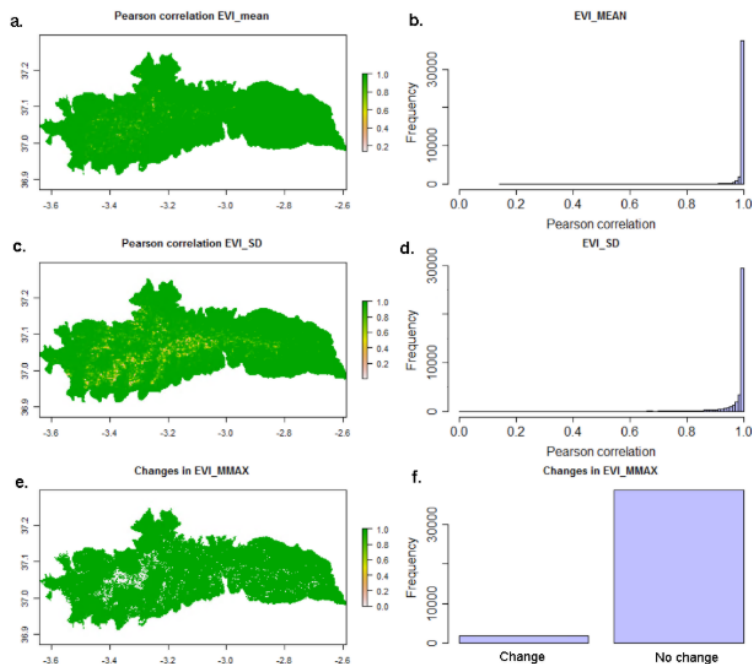
Figure 2. Comparisons of EFAs with MODIS MOD13Q1 EVI data filtered by quality (layer product
"QA summary": bands 2 (snow/ice) and 3 (clouds)) and with pre-processing data of the product and
negative values (generally corresponding to snow, ice or water) converted into zeros. Left panels (a, c,
e) show maps of simple sliding window (3x3 pixels) correlation for EVI_mean and EVI_SD
(continuous variables) and changes for EVI_DMAX (discrete variable). Right panels (b, d, f) show
the histograms associated with the left panel maps, i.e. how many pixels have a low or high
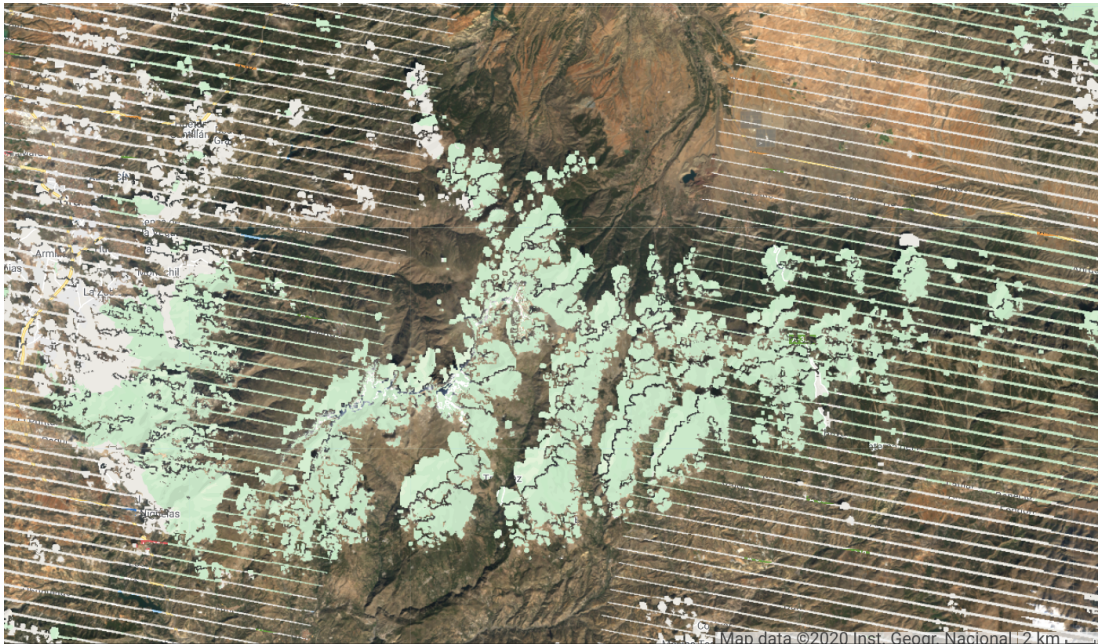correlation (b, d) and for the case of EVI_DMAX how many pixels have changed or not (f).

Fig. 2.
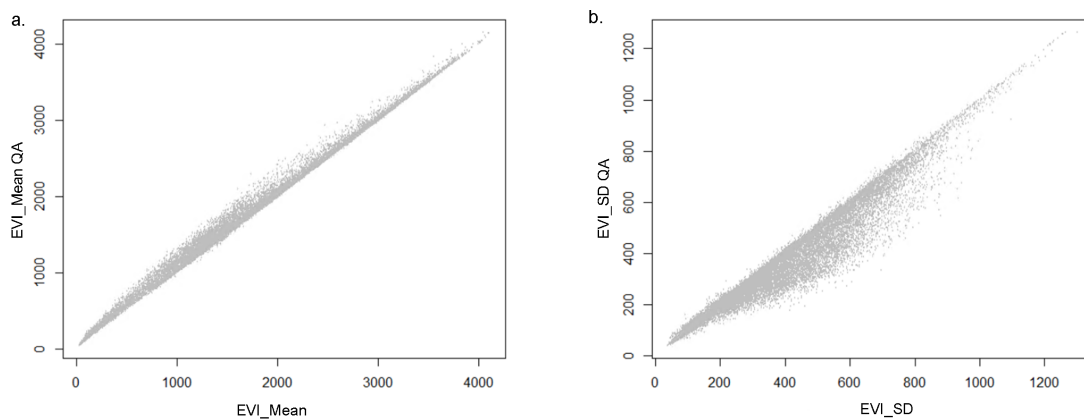
Fig. 3. Scatter plots between the non-filtered (X-axes) and filtered (Y-axes) EFAs: a) EVI_mean MOD13Q1.006 and b) EVI_SD MOD13Q1.006, both of the average year.

Fig. 4. Effect of Scan Line Corrector fault on Landsat7 imagery in Sierra Nevada and data gaps due to clouds (in green and white). Landsat-7 image courtesy of the U.S. Geological Survey.
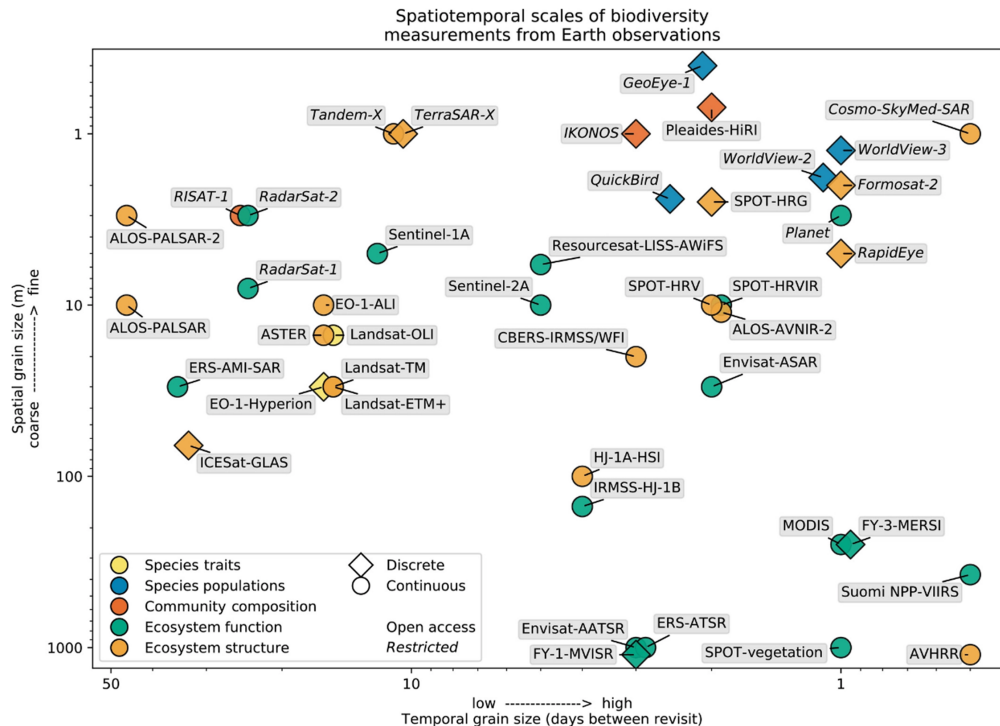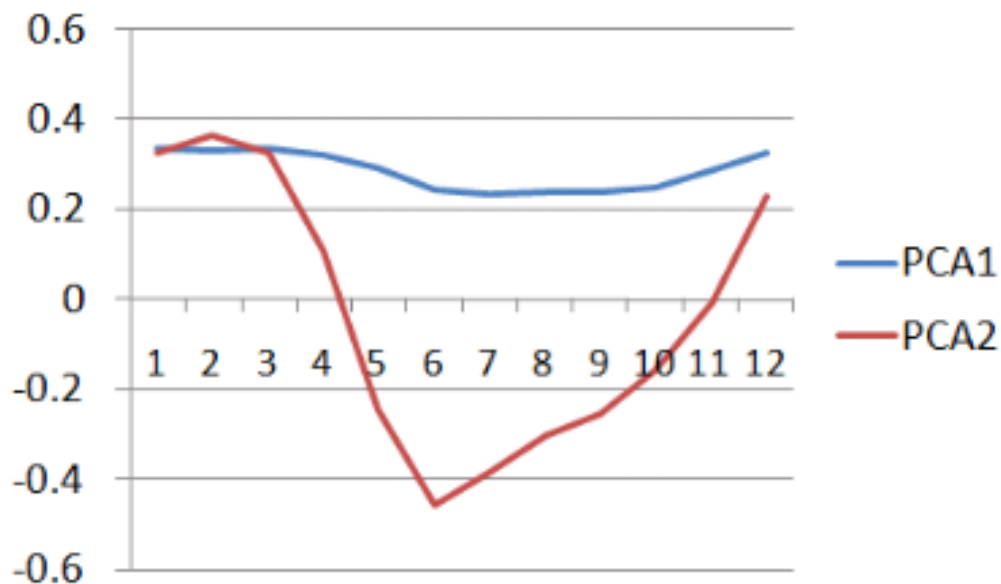
C23

Figure 5. Anderson (2018) : *"Log–log plot of spatial and temporal and grain sizes for 44 current and historic satellite Earth observation (EO) sensors, coloured by biodiversity pattern type. Several sensors have been used to measure multiple biodiversity patterns, and the most cited or most novel were selected in these cases".*

Fig. 5.

Fig. 6. Eigenvectors of the first two components of a PCA performed on the annual curve of EVI values in Sierra Nevada (Axis x: months; axis y: eigenvectors values).
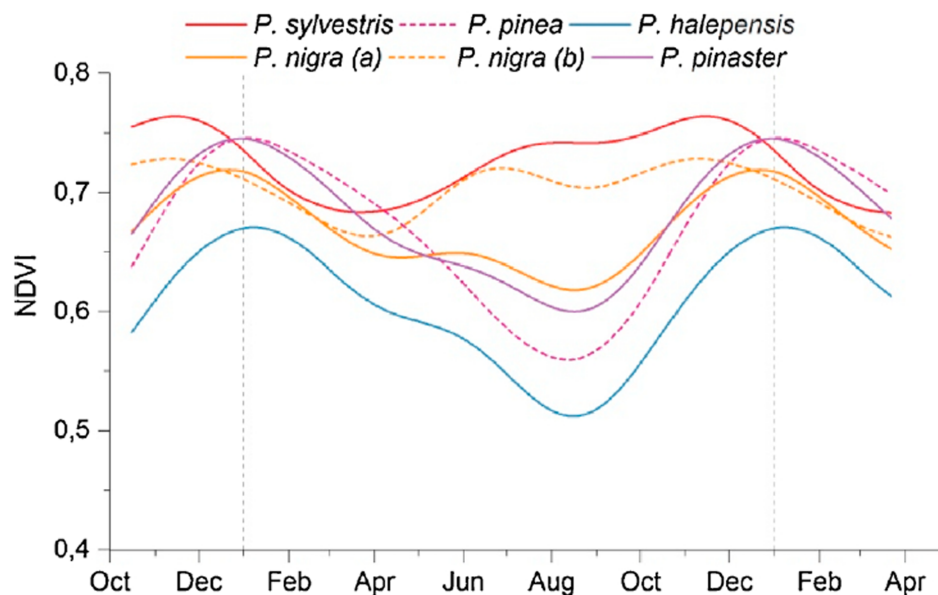
Figure 7. From Aragonés et al. (2019). "*NDVI values in the average year. This shows the average values of the sum of the trend and seasonal components for each species, obtained using the BFAST algorithm. Three months of data are shown before and after, as the growing seasons can span the calendar year.*" This study was carried out in the Iberian Peninsula, including samples from Sierra Nevada.
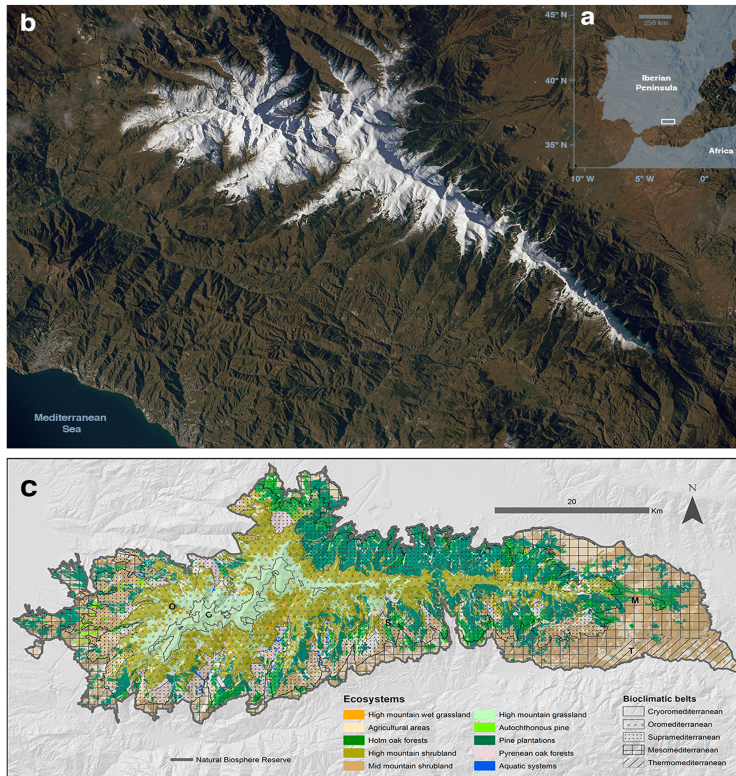
Fig. 7.

Figure 1. Study area: Sierra Nevada Biosphere Reserve. a) Location in the context of the Iberian Peninsula; b) remote view of Sierra Nevada mountain region (image from the International Space Station took in December 2014; courtesy of "Earth Science and Remote Sensing Unit, 615 NASA Johnson Space Center"); c) delimitation of the Biosphere Reserve and the distribution of the main ecosystems (Pérez-Luque et al. 2019) and thermotype bioclimatic belts (Molero-Mesa and Marfil 2015).

Fig. 8. NEW FIGURE 1 OF MANUSCRIPT

						Scores						
PCA axis	%[a]	Jan	Feb	Mar	Apr	May	Jun	Jul	Aug	Sep	Oct	Nov	Dec
1	87.3	0.334	0.328	0.333	0.318	0.293	0.246	0.236	0.239	0.242	0.251	0.287	0.325
2	96.5	0.329	0.365	0.326	0.109	-0.244	-0.454	-0.380	-0.301	-0.252	-0.154	-0.007	0.229

[a] *Cumulated variance*

Fig. 9. Table 1. Eigenvectors and cumulative variance explained by the first two components of a principal component analysis (PCA) performed on the annual curve of EVI values in Sierra Nevada.

	PC1	PC2
EVI_Mean	0.94	-0.01
EVI_SD	-0.14	-0.75
DMAX_Sine	-0.10	0.67
DMAX_Cosine	0.017	-0.61

Fig. 10. Table 2. Correlation values between PCA axis 1 and 2 and ecosystem functional attributes.

Printer-friendly version

Discussion paper

	EVI_Mean	EVI_SD
EVI_Mean	1	
EVI_SD	-0.14	1
EVI_DMAX	0.10	-0.05

Fig. 11. Table 3. Pearson correlation values between metrics.

Interannual variability	n pixels	% study area surface	Cumulated % of study area surface
1	49	0.12	0.12
2	301	0.74	0.86
3	2582	6.32	7.17
4	4436	10.85	18.02
5	6010	14.70	32.73
6	6605	16.16	48.88
7	6064	14.83	63.72
8	5144	12.58	76.30
9	3875	9.48	85.78
10	2707	6.62	92.40
11	1678	4.11	96.51
12	871	2.13	98.64
13	372	0.91	99.55
14	130	0.32	99.87
15	40	0.10	99.97
16	12	0.03	99.99
17	2	0.01	100.00

Fig. 12. Table 4. Number of pixels and percentage of the study area that experienced different levels of inter-annual variability in EFTs (number of EFTs that were observed over the period in each pixel).